NEW CONCEPTS FOR SPACECRAFT ANTENNAS AND RADAR STRUCTURES BASED ON ULTRA-THIN COMPOSITES

Sergio Pellegrino
Department of Engineering, University of Cambridge,
Trumpington Street, Cambridge, CB2 1PZ, U.K.

ABSTRACT

This paper presents a new deployable reflector concept for an Earth observation mission that requires a low-cost L-band Synthetic Aperture Radar (SAR) instrument with a large aperture. A novel "hollow solid" structural concept is proposed that comprises curved surfaces formed from thin sheets of carbon-fiber-reinforced-plastic connected by flexible hinges along the edges. The front surface of the hollow solid provides the reflective surface. This proposed structure has very high stiffness-to-mass-ratio, because of its thin-walled box-type construction. A detailed study of a half-scale technology demonstrator, including design, manufacture and testing, is presented in the paper.

INTRODUCTION

This paper presents a novel deployable reflector structure for a mission requiring a low-cost L-band Synthetic Aperture Radar (SAR) instrument. This comprises an offset parabolic cylinder with a linear feed array. The satellite in its flight configuration and SAR imaging orientation is shown in the schematic diagram of Figure 1. This configuration provides some of the advantages of phased arrays (like low loss and elevation beam steering), at much reduced cost. The required reflector shape is an offset parabolic cylinder with an arc-length of 7.9 m and width of 3.2 m. The reflector structure is connected to the spacecraft bus by a truss structure, which would be deployed before the reflector structure; this structure will not be discussed in the paper.

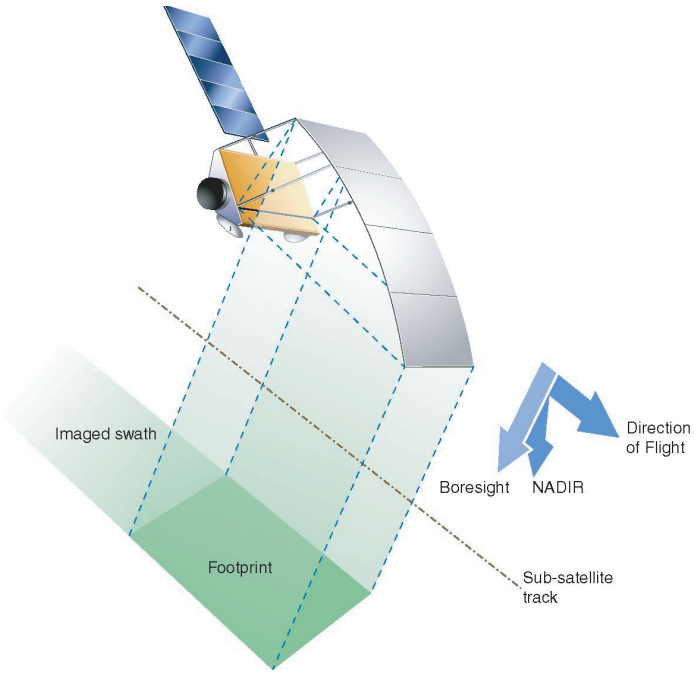

Figure 1: Flight configuration (courtesy of EADS Astrium).

A novel structural concept for this application is presented. The idea is to form a “hollow solid” from thin, curved sheets of carbon-fiber-reinforced-plastic (CFRP), connected by flexible hinges along the edges. One face of the hollow solid has the required shape for the reflector. This structure has very high stiffness-to-mass-ratio, because of its thin-walled box-type construction. Only minimal use of stiffening elements is required, as the curvature of each surface is an effective way of increasing the local buckling stress of a very thin sheet.

A brief outline of the paper is as follows. First we explain the proposed approach, then we derive the cutting pattern for the four sheets that make up the structure. Then, we outline the key stages of the design process of this novel structure, including the constraints imposed by the requirement to elastically fold the structure, and the preliminary design of a full-scale flight structure. The design and construction and laboratory testing of the half-scale demonstrator are presented. A discussion concludes the paper.

STRUCTURAL CONCEPT

The key geometric ideas behind the proposed new concept can be explained as follows.

Consider a flat sheet A with a curved edge, connected to a coplanar, flat sheet B with a matching curved edge, as shown in Figure 2(a). If sheet A is rotated through 90°, both sheets become curved, as shown in Figure 2(b).

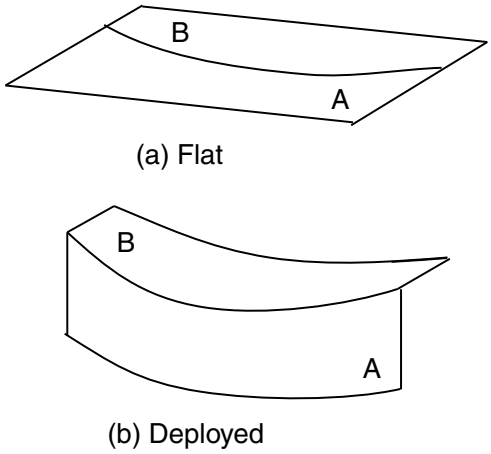

Figure 2: Use of a shaped sheet A to shape sheet B into a singly-curved surface.

Next consider the “hollow-solid” structure shown in Figure 3, made by connecting two pairs of identical flat sheets. Sheets A and A’, which are identical, are connected to sheets B and B’, also identical. The curved edges are identical in all four sheets. In the configuration shown in Figure 3(b) the four sheets form curved surfaces which define a hollow solid, whose shape is defined by the cutting pattern of the sheets. The folded configuration shown in Figure 3(a) is obtained by introducing fold lines in the middle of sheets A and A’ (shown as broken lines in Figure 3(b)).

Once the hollow solid structure has been flattened (which we will call stage one of the folding process), it can then be folded longitudinally (which we will call stage two of the folding process) as an accordion.

The required reflective surface is obtained by replacing sheet B with a rectangular sheet, see

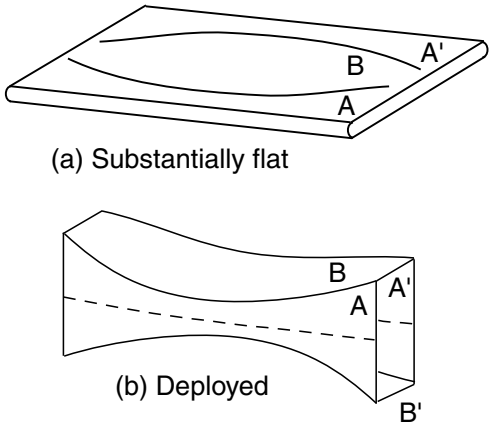

Figure 3: Hollow solid structure.

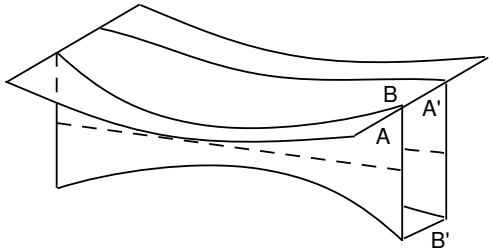

Figure 4: Antenna structure in deployed configuration.

Figure 4.

Next, we explain how to determine the edge profile of sheet A. Figure 5(a) shows two cylindrical surfaces, A and B, that intersect along the three-dimensional curve OEC. Surface B can be generated by considering the two-dimensional curve $z = d(x)$, and by translating this curve along a generator segment, e.g. EM, parallel to the y-axis. Note that in Figure 5(a) a general point on $z = d(x)$ is point D; also note that the x-axis starts at the origin O and passes through the end point C of the curve. Finally, note that all points on EM have the same arc-length distance s from the y-axis, and the same distance d from the xy plane.

Let F and G be the projections of D and E onto the xy plane, clearly

$$\overline{\mathrm{DF}} = \overline{\mathrm{EG}} = d \tag{1}$$

Now consider flattening the surface B onto the xy-plane, without moving its edge along the y-axis. During this process EM moves in both x and z directions, while remaining parallel to the y-axis. The distance d of E from the xy-plane becomes zero.

Next, we consider the additional conditions that need to be satisfied for the two surfaces, A and B, to be flattened together. We look for the locus of points E on the surface B defining the curved profile of surface A, and hence the curve along which the two surfaces intersect. It will be assumed that the generator EM is perpendicular to the surface A in the curved configuration (i.e. the deployed configuration), although a more general situation could be considered. It will also be assumed that the two surfaces are tied to each other at the general point E and there is no relative motion of the tie points when the surfaces are flattened.

The following conditions apply

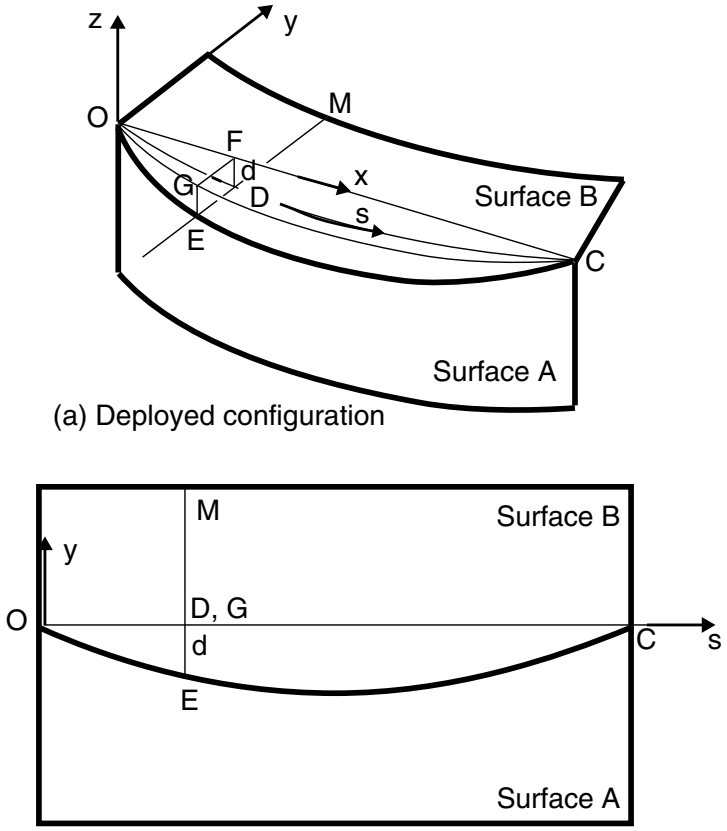

Figure 5: Edge profile of sheet A.

- Condition 1: The arc-length of OE, measured along surface B, is equal to the arc-length of OE measured along surface A.
- Condition 2: When the surfaces are flattened, both points D and G move towards point F, and so D and G coincide when the surfaces are flattened, see Figure 5(b). Hence, it follows that

$$\overline{\mathrm{DE}} = \overline{\mathrm{EG}} = d \tag{2}$$

In conclusion, given a cylindrical surface (surface B) defined by the curve $z = d(x)$, first one has to determine the arc-length, $s(x)$, along the curve and then one has to determine the edge profile of surface A, given by $d(s)$. Note that $d(s)$ also defines the curve along which surface A is to be connected to surface B. If $d(s)$ cannot be found explicitly, then an implicit description in terms of $s(x)$ and $d(x)$ can be used instead.

Note that it follows from Equation 2 that the two sheets form identical cylindrical surfaces, i.e. with equal diretrix.

CUTTING PATTERN

Here we work out the cutting pattern for the sheets of a reflector structure, to provide the required focal length, aperture, and offset distance.

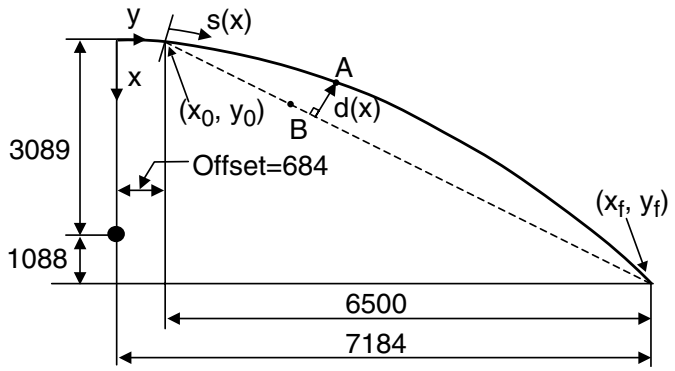

Figure 6: Profile of RF surface (dimensions in mm).

The required parabolic profile for the reflective surface is shown in Figure 6. The cutting pattern of the flat sheets requires the arc length $s(x)$ and the perpendicular distance from the chord line to the parabola $d(x)$ to be worked out, as discussed in previous section.

The equation of a parabola with vertex at (0, 0) is given by

$$y^2 = 4ax \tag{3}$$

where a is the focal distance. The arc length from the offset (x_0, y_0) to a generic point A(x, y) on the parabola, is calculated from

$$s(x) = \int_{x_0}^{x} \sqrt{1 + (dy/dx)^2}\, dx \tag{4}$$

Substituting Eq. 3 into Eq. 4 and carrying out the integration yields

$$\begin{aligned} s(x) = \quad & \sqrt{x\,(x+a)} - \sqrt{x_0\,(x_0+a)} \\ & + \frac{a}{2}\ \ln \frac{2\,x + a + 2\,\sqrt{x\,(x+a)}}{2\,x_0 + a + 2\,\sqrt{x_0\,(x_0+a)}} \end{aligned} \tag{5}$$

The equation of the chord line of the reflector, which joins the start point (x_0, y_0) and end point (x_f, y_f) of the reflective surface, is written as

$$y_c = a_0 + a_1 x \tag{6}$$

where $a_0 = (y_0 x_f - x_0 y_f)/(x_f - x_0)$, and $a_1 = (y_f - y_0)/(x_f - x_0)$.

Consider a general point on the chord line, B(x_c, y_c). The distance between A and B is

$$d_{AB} = \sqrt{(x - x_c)^2 + (y - y_c)^2} \tag{7}$$

Substituting Eqs. 3 and 6 into Eq. 7 we obtain

$$d_{AB} = \sqrt{(x - x_c)^2 + (2\sqrt{ax} - a_0 - a_1 x_c)^2} \tag{8}$$

The shortest distance $d(x)$ from point A to the chord line can be obtained by minimizing d_{AB}. Hence we set the first derivative of d_{AB} with respect to x_c equal to zero and solve for x_c, to obtain

$$x_c = \frac{(x + 2a_1\sqrt{ax} - a_0 a_1)}{(1 + a_1^2)} \tag{9}$$

The shortest distance $d(x)$ is obtained by substituting Eq. 9 into Eq. 8

$$d(x) = \frac{|\,(x\ a_1 + a_0 - 2\,\sqrt{ax})\,|}{\sqrt{1 + {a_1}^2}} \tag{10}$$

The cutting pattern for the flat sheets, defined by $s(x)$ and $d(x)$ in Eqs 5, 10, is shown in Figure 7.

Two more parameters are needed to completely determine the cutting pattern for the reflector, namely the distance between the two matching profiles in each of the four sheets that form the hollow solid. These parameters are determined by thinking about the size of the packaged structure and by optimizing the performance of the structure in the deployed configuration [1].

DESIGN FOR FOLDING

The reflector structure is to be constructed from thin sheets of CFRP. This section presents the analysis and detailed testing of those elements of the reflector structure that need to elastically deform in order to allow folding of the structure.

Connections

Two types of connections have been used, see Figure 8. These connections have been made with adhesive tape in order to provide a uniform stress distribution across the two sheets being connected.

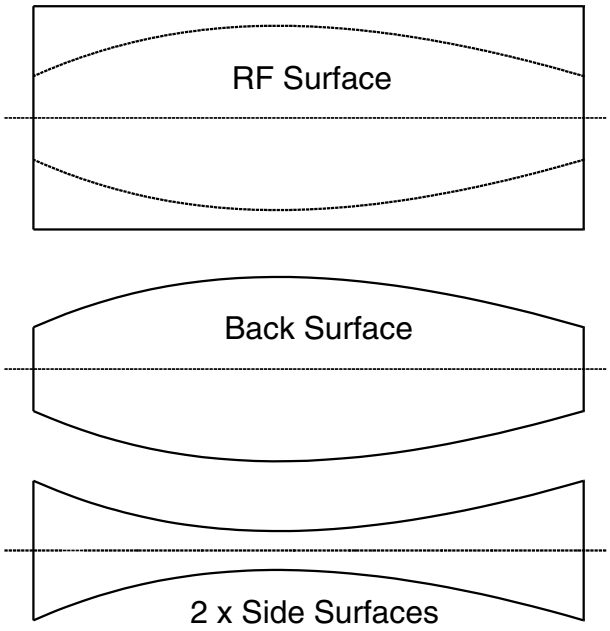

Figure 7: Cutting pattern for reflector structure.

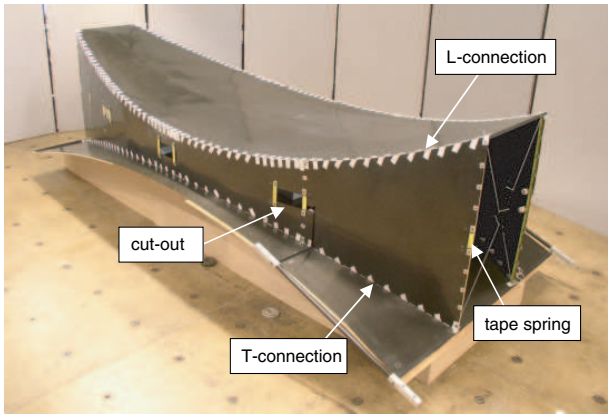

Figure 8: Types of connection.

Elastic Hinge Lines

Elastic hinge lines are formed between parts of a sheet of CFRP that describe an essentially rigid-body rotation with respect to each other. Careful design of the parts of the structure that have to flex is required, limiting the maximum curvature to which they are subjected. In simple terms, the maximum strain imposed by the folding process has to be smaller than a threshold value, which depends on the properties of the CFRP sheet.

An elastic hinge line is made to latch in one particular configuration by fastening tape springs (lengths of steel carpenter tape were used for the demonstrator, but CFRP tape springs have been subsequently developed) to it. Note that in Figure 8 a small part of the sheet under each tape spring has been removed to form a cut-out which provides the clearance needed for the tape springs to fold without being overstressed.

Bending tests were carried out to measure the minimum radius of curvature prior to failure of laminated plates. Because of their small thickness, these plates can be bent into very small

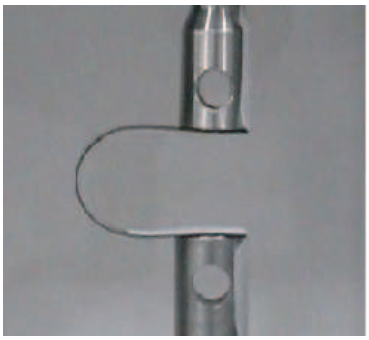

Figure 9: Bending test for thin composites.

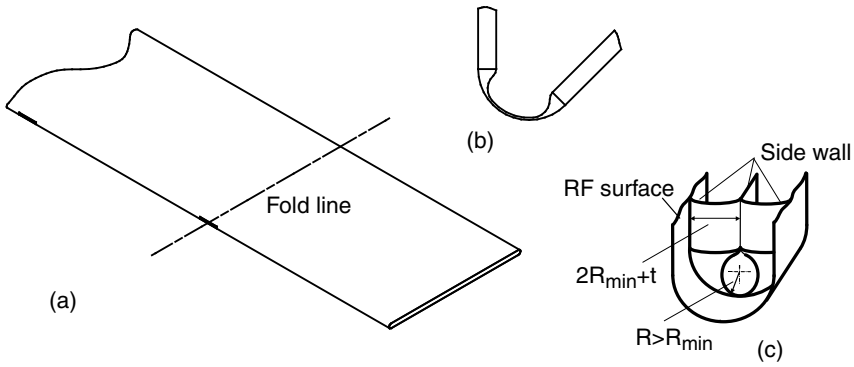

Figure 10: Stage two of folding process; (a) isometric view of flattened reflector; (b, c) views of partially and fully-folded folded transverse hinge line.

radii, and hence standard three-point and four-point bending tests are unsuitable to measure the minimum bend radius. An alternative test that allows large displacements was devised, see Figure 9. Strip specimens with a width of 15 mm are attached to circular rods with a diameter of 15 mm, in turn connected to an Instron materials testing machine. The specimens are $\pi R_i + 30$ mm long, where R_i is an initial estimate of the minimum radius of curvature, in order to ensure that failure takes place roughly in the configuration shown in the figure.

The tests were recorded with a digital video camera. Once the specimen had failed, the minimum bend radius was measured using one or more images captured just prior to failure. If the specimen is too long, its ends come into contact prior to failure and in this case the test needs to be repeated using a shorter specimen. See Ref. [2] for more details.

Sizing of Cut-outs in Side Walls

Cut-outs are required to reduce the maximum strain in the region where two fold lines cross. It is desirable for these cutouts to be as small as possible, to reduce the loss of stiffness of the structure. A rectangular shape (with rounded corners) of width w and length L was adopted.

The width, w, of a cut-out has to be such that the sidewall can be bent 180° along a longitudinal fold line; this requires

$$w \geq \pi R_{min} \tag{11}$$

to prevent material failure, where R_{min} is the minimum bend radius of the side wall.

The length of the cut-out is determined by considering a 180° transverse fold, Figure 10(a), in

the already flattened reflector structure. Assuming that the side walls and the RF surface have the same thickness and material properties, and hence the same minimum radius of folding R_{min}, the length of the cut-out can be estimated from

$$L \geq 2\pi R_{min} + \pi \mathrm{t} \tag{12}$$

Note that the part of the side wall that lies on the inside of the fold needs to bend first in one sense and then in the opposite sense. If the radius of curvature is assumed to be R_{min} everywhere, the inner part of the side wall would interfere with the outer part; however this can be eliminated by considering a fold with a non-uniform radius.

DESIGN AND TESTING OF DEMONSTRATOR

A half-scale structure that can be tested in the laboratory without complex gravity compensation, was designed.

A T300/LTM45 plain weave CFRP, 3-ply laminate (0/45/0) with uniform thickness was adopted. R_{min} was set at 24 mm, which provides a margin of 2.3 on material failure, in the folded configuration.

Each side wall has three windows whose dimensions are, from Equations 11 and 12, 210 mm long by 75 mm wide. The ends of the structure are stiffened by thin walled square section stiffeners (10 mm wide, 0.5 mm thick) made of the same material.

A preliminary finite element analysis indicated that this structure is prone to buckle into a mode involving localised deformation of the upper part of the side wall, between the third cut-out and the tip. This mode was stiffened by attaching steel tape springs to both edges —for symmetry— of the side walls. Additional stiffening of the side walls was provided by attaching tape springs to the edges of all the cut-outs. The total mass of the demonstrator was estimated at 7.2 kg.

A detailed design of the demonstrator was then prepared; the CFRP sheets and angle stiffeners were constructed and water-jet cut by Brookhouse Paxford Ltd; all fixtures were made of Aluminium-alloy in the Workshops of the Engineering Department; the tape springs were made by cutting suitable lengths of Sears steel tape measure; 48 mm high cup-and-cone spacers made of a structural foam were made for the side walls, on either side of each hinge line; and all connections were made with 3M 79 woven-glass tape and 3M Scotch-Weld DP490 epoxy resin. The structure was then assembled in the the Deployable Structures Laboratory at Cambridge University. Its total mass was 11 kg, due to the mass, previously unaccounted for, of all spacers, washers, nuts and bolts, etc. Further details on the parts and assembly process are available in a technical report [1].

The reflector structure, see Figure 11, was attached through an interface frame to a tubular steel support structure, with a 2.5 kg single-point gravity offload at the root of the back surface, and a 4 kg offload connected to the top edge of the RF and back surfaces, through a horizontal bar.

Measurements of surface accuracy and stiffness were then taken, in the deployed configuration. The stiffness of the demonstrator was measured before packaging, whereas the surface accuracy was measured both before packaging and after deployment.

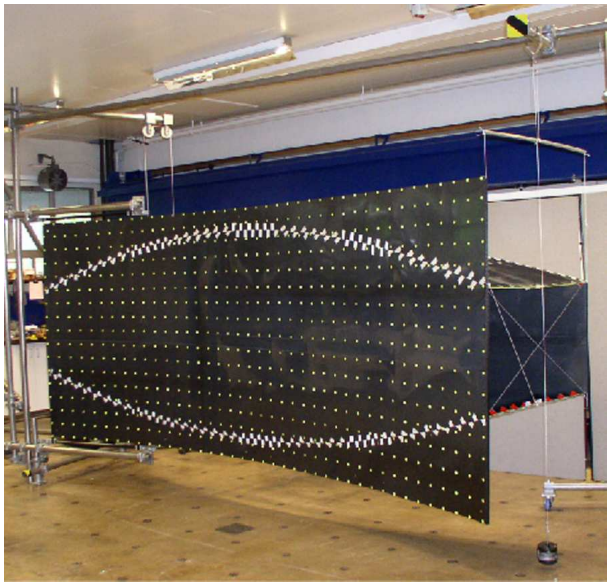

Figure 11: Half-scale demonstrator attached to support rig and with gravity off-load at the tip.

Measurements of Stiffness

Displacement measurements of the tip of the structure were carried out in the deployed configuration. These measurements were taken with a LK 081 (Keyence Co.) laser displacement sensor.

Static loads in the out-of-plane and transverse directions were applied to the tip of the reflector structure, by means of a string and pulley system. The displacements in the direction of the load were measured in each test, and in each case a linear best-fit relationship was obtained, in order to estimate the stiffness of the structure for the both load cases. Figures 12 and 13 compare the measured response to the results from an ABAQUS linear-elastic static analysis. The ABAQUS model is stiffer in both cases, by 15% in the out-of-plane direction, and by 49% in the vertical direction.

Obviously, some refinement of the model (e.g. by measuring the actual elastic properties of the composite sheets and by modelling the support conditions in more detail) would be desirable. However, note that the out-of-plane stiffness of the structure, which is the lowest one, is in good agreement with the measurements.

Measurement of Surface Accuracy

A PC based photogrammetry package, PhotoModeler Pro 4.0 [3], was used to measure the surface accuracy of the RF surface of the half-scale demonstrator. 680 circular, equally spaced targets, were attached to the surface. The measurements were carried out both before packaging the structure for the first time and after deploying it.

Since we are dealing with a parabolic cylinder, the problem is essentially in two dimensions. The z-coordinates of the target points, where z is perpendicular to the plane of the parabola, see Figure 6, can be disregarded. The equation of the best-fit parabola, in a coordinate system in which X and Y are parallel to x and y, respectively, and X_0 and Y_0 are the measured coordinates

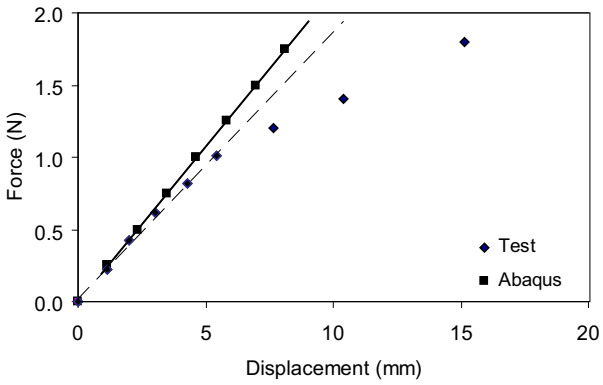

Figure 12: Response to horizontal tip loads.

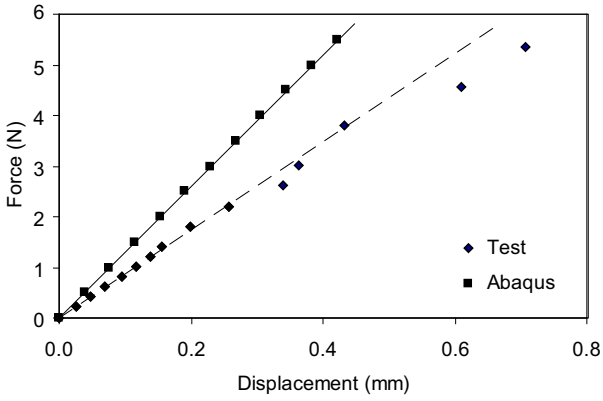

Figure 13: Response to vertical tip loads.

of the vertex of the parabola, is

$$X = \frac{1}{4a^*}Y^2 - \frac{Y_0}{2a^*}Y + \left(X_0 + \frac{Y_0^2}{4a^*}\right) \tag{13}$$

Note that, once the best fit parabola in Eq. 13 has been obtained, the focal length is a^*.

For n target points that are equally spaced on the surface, the root mean square (RMS) error in the axial direction X, with respect to the best fit parabola, is calculated from [4]

$$\delta_{ex} = \sqrt{\frac{\sum(\hat{X}_i - X_i)^2}{n}} \tag{14}$$

where $\hat{X}_i$ is the axial coordinate of a general target point and X_i is the corresponding axial coordinate of the best fit parabola.

Before packaging, the best-fit focal length was $a^* = 1550$ mm, which is very close to the design focal length of $a = 1544.5$ mm. The RMS error of the target points from the best fit parabola was 3.8 mm. It was noticed that the points near the upper edge of surface, between the two stiffeners that form the longer edges of the interface frame, yielded higher errors. It was thus realised that the interface frame and the RF surface had not been not correctly aligned during assembly. When this misalignment was corrected, the RMS error reduced to 3.0 mm.

The surface accuracy measurements were repeated after packaging and deployment of the structure. The best-fit focal length was 1547.1 mm. The total RMS error from the best fit parabola remained unchanged.

PACKAGING AND DEPLOYMENT OF THE DEMONSTRATOR

Packaging

Packaging consists in flattening the structure and then introducing three transverse folds that allow it to fold into an accordion. The folding sequence is shown in Figure 14.

Flattening the structure involves bending the side walls through 180°. The process through which this happens needs to be carefully controlled, to prevent damaging the structure. First, the demonstrator was placed on a plywood mold, with the RF surface facing down and the back surface facing up. Foam plugs that fit snugly inside the “hollow solid” were placed inside the structure to prevent it from suddenly collapsing. Easy-release cable ties were passed through corresponding sets of cup-and-cone spacers, and were tied to take up any slack.

Next, flattening of the structure was initiated by pulling the side walls outwards with a pair of wooden poles placed inside the structure, between the sets of cup and cone spacers. Each pole was loaded, through a cable and pulley system, with counter weights, while the foam plugs were slowly pulled out to allow the back surface to come down.

Note that as the structure flattens the back surface and the RF surface need to move symmetrically, respectively upwards and downwards, to keep the longitudinal fold lines in the sidewalls straight and horizontal. To ensure this, plywood sheets were gradually pushed between the mold and the structure, and slowly raised at the far ends, to move the RF surface upwards.

It was discovered that the structure has a tendency to “roll-over”, i.e. to slew sideways during folding. This was avoided by cross-bracing both ends with cable ties attached to adjustable

plastic ties, which are held taut at all times. Also, two people held the upper ends of the back surface.

Once the back surface had stopped coming down under its own weight, weights were added on top of expanded polystyrene sheets to bring the back surface down. Throughout this process the easy release cable ties were progressively tightened to take up any slack, and the foam plugs were gradually pulled out from either end. Once the demonstrator had substantially flattened, plastic ties were introduced at 150 mm spacing along the fold line of the side walls.

Longitudinal folding is much simpler than flattening. First, the two end sections are rotated through 180°, making sure that the RF surface ends up on the outside, and then the middle fold is introduced, this time placing the RF surface on the inside.

Figure 15 shows the the packaged structure, whose outer envelope is 1700 mm long, 950 mm wide, and 260 mm high. Note that the packaged envelope of the full-scale, flight structure would have the same height, but double the length and width.

Deployment

It is planned to deploy this structure by cutting all the restraints and then releasing the structure by slowly paying out a tether. However, this could not be demonstrated because the side surfaces of the demonstrator are too thick and hence store an excessive amount of strain energy stored for all longitudinal and transverse constraints to be released at once. Instead, an operator assisted deployment was carried out.

The packaged structure was attached to a tubular steel support structure, through the corners of the rectangular interface frame. The structure was then deployed under quasi-static conditions, in two stages, with gravity supports provided along the three transverse fold lines.

The photographs at the start of the sequence in Figure 16 show the first stage of the deployment process, in which the structure deploys as an accordion and ends up flat. Friction in the gravity offload system held the structure in equilibrium in any of its intermediate configurations.

Once the first stage of the deployment process had been completed, the side walls were allowed to unfold by gradually releasing the cable ties, thus separating the RF surface from the back surface. The structure was cross-braced at both ends to prevent it from slewing.

CONCLUSION

An innovative concept for large deployable reflectors for synthetic aperture radar applications has been presented. This concept can deliver a parabolic profile of high accuracy with a structure of very low mass, high stiffness, and potentially very low cost.

At full scale, i.e. for a reflecting surface that is 7.9 m long and 3.2 m wide, it has been estimated that the proposed approach would lead to a structure with a mass of about 33 kg, which is two-and-half times lighter than a traditional reflector structure made from lightweight, curved panels with self-locking hinges.

The new concept is based on forming a collapsible hollow solid, defined by four cylindrical surfaces. These surface are formed from thin-walled CFRP sheets hinged along their edges. This is just one particular approach, and it should be noted that there are many other ways of

Figure 14: Packaging sequence, from top left to bottom right.

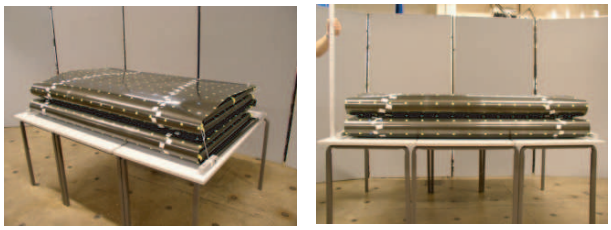

Figure 15: Packaged demonstrator.

implementing this type of structural concept. Patent applications protecting the new concept presented in this paper have been filed [5].

The key to forming a cylindrical surface with the required shape lies in the cutting pattern for the edges of the sheets. A general methodology for determining the cutting pattern has been presented, and for the case of parabolic shapes an analytical expression for the cutting pattern has been obtained, in terms of the focal length, aperture and offset distance of the reflector.

The proposed concept has been demonstrated by designing, constructing and testing a half-scale physical demonstrator made from 0.3 mm thick CFRP sheets, which would also be used for the full-scale structure. This model has achieved a surface accuracy of 3.0 mm RMS, typical mass of 1.7 kg/m^2, and packaging density of 1/20th of deployed volume.

ACKNOWLEDGMENTS

This research was funded by EADS Astrium Ltd, under the BNSC Newton scheme. An earlier version of this paper, co-authored with P. Howard, O. Soykasap, and A.M. Watt, was presented at the 28th ESA Antenna Workshop on Space Antenna Systems and Technologies, held on 31 May-3 June 2005 at ESTEC, Noordwijk, The Netherlands.

References

[1] Soykasap, Ö., Pellegrino, S., Deployable Synthetic Aperture Radar Reflector, CUED/D-STRUCT/TR209, Department of Engineering, University of Cambridge, 2004.

[2] Yee, J.C.H, and Pellegrino, S., Folding of woven composite structures, *Composites/A*, 36(2), 273-278, 2005

[3] PhotoModeler Pro 4.0, User Manual, Eos Systems Inc, Canada, 2000.

[4] Levy, R., Structural Engineering of Microwave Antennas, The Institute of Electrical and Electronics Engineers, New York, 1996.

[5] Watt, A.M., Pellegrino, S., Howard, P., Improvements Relating to a Deployable Support Structure, Patent Applications: UK-GB0316734.3, European-EP03254474.4, 2003.

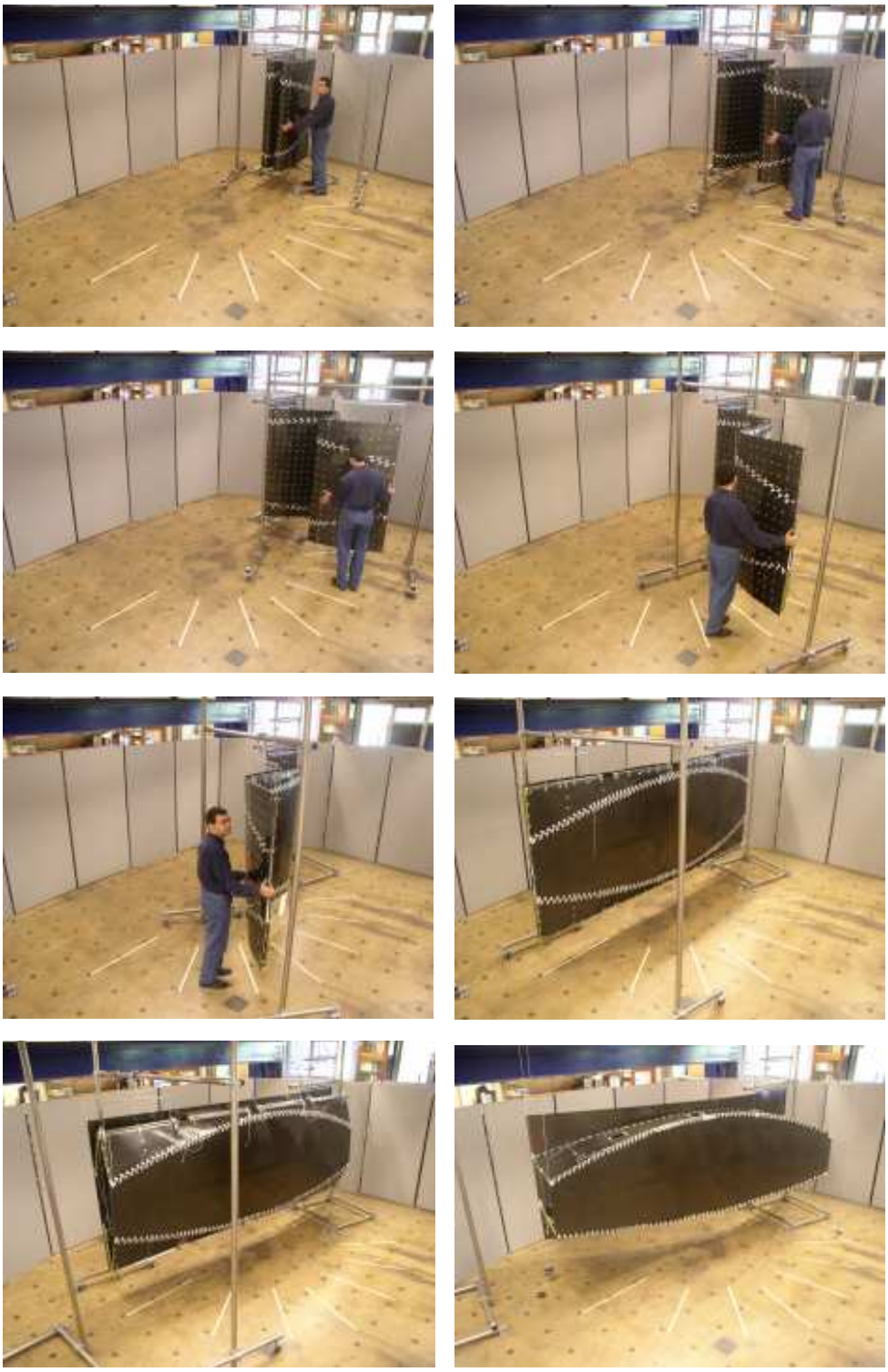

Figure 16: Deployment sequence, from top left to bottom right.